Internal Motion of Deoxyribonucleic Acid in Chromatin. Nanosecond Fluorescence Studies of Intercalated Ethidium†

Ikuo Ashikawa, Kazuhiko Kinosita, Jr., Akira Ikegami,* Yoshifumi Nishimura, Masamichi Tsuboi, Kazutada Watanabe, Koujiro Iso, and Takashi Nakano

ABSTRACT: We have investigated the internal motions of DNA in a nucleosome core particle and chromatin by measuring the nanosecond fluorescence depolarization of intercalated ethidium. Assuming that the observed anisotropy decay originates from the torsional motion of DNA, we have analyzed the dynamics of DNA in a nucleosome core particle and in chromatin in detail. The results suggest that DNA in a nucleosome core particle has a torsional rigidity similar to that of DNA in solution and that even at the point of the ionic bonds between DNA and a histone octamer the torsional motion of DNA is not completely inhibited. On the other hand, the dynamics of linker DNA in chromatin were found to reflect the overall structural state of the chromatin: the motion of linker DNA was suppressed as the structure of chromatin turned from an extended state to a condensed one. This indicates that, in solenoidal chromatin, nucleosome movements in chromatin are largely suppressed. Furthermore, the result may suggest that the torsional rigidity of linker DNA is increased as it is forced to bend in solenoidal chromatin.

Recently, the dynamics of B-form DNA in solution have been studied extensively by using techniques such as NMR (Early & Kearns, 1979; Hogan & Jardetzky, 1979, 1980b; Bolton & James, 1980; Opella et al., 1981), fluorescence depolarization (Wahl et al., 1970; Thomas et al., 1980; Millar et al., 1980, 1982), electron spin resonance (ESR) (Robinson et al., 1980), and triplet anisotropy decays (Hogan et al., 1982). DNA experiences subnanosecond motions around its phosphate backbone moiety, according to observations by ^{31}P NMR (Bolton & James, 1980; Opella et al., 1981). Fluorescence anisotropy studies (Thomas et al., 1980; Miller et al., 1980, 1982) of intercalated dyes and ESR studies of intercalated spin-labels (Robinson et al., 1980) have revealed motions in the nanosecond range. Furthermore, a recent triplet anisotropy study has shown the presence of internal motions of DNA in the microsecond region (Hogan et al., 1982).

Several studies have already been carried out which used the anisotropy decay of ethidium bromide, a fluorescent dye which can be intercalated in DNA firmly. Barkley & Zimm (1979) assumed DNA to be a uniform elastic rod and calculated theoretically the anisotropy decay curve of intercalated ethidium bromide. They showed that the decay in the nanosecond range is caused mainly by the torsional motion of the DNA rod. In their paper, they concluded that the anisotropy decay curve would be of the form $\exp(-at^{1/2})$, where a is a constant. Independently, Allison & Schurr (1979) assumed that DNA consists of a series of $N + 1$ identical rigid rods connected at their ends by torsion springs and calculated the anisotropy decay curve of intercalated ethidium more rigorously by using a more general model, specifically allowing finite contour lengths, arbitrary subunit lengths, and a random distribution of bound dye. They also concluded that the anisotropy decay is of the form $\exp(-at^{1/2})$ except at $t \approx 0$. These predictions were first verified by Thomas et al. (1980), and independently by Millar et al. (1980), using picosecond fluorescence measurements of intercalated ethidium. Millar et al. (1982) estimated torsional rigidities of various kinds of DNA and RNA and tabulated the results.

How these motions, particularly the torsional motion, change when DNA complexes with proteins is an interesting problem. In a nucleus of eucaryotes, DNA exists as chromatin (Kornberg, 1977), which is a complex of DNA and histone proteins, and the mode of interaction between these two substances is presumed to influence the gene expression by some yet unknown mechanism. The dynamics of the phosphate moiety of the DNA backbone in a core particle have been studied already by the ^{31}P NMR technique (Klevan et al., 1979; Shindo et al., 1980), and, according to these studies, motions of phosphates are not largely suppressed even when DNA is wound around the core protein. Allison et al. (1982) and Schurr (1982) have developed the theories which related ^{31}P NMR relaxation to the movements of the DNA rod. On the other hand, Hogan & Jardetzky (1980a) indicated complication of the relation between the movements of the DNA rod and the motions observed by NMR. We think that observation of the anisotropy decay of intercalated ethidium provides the most direct information about the movements of the DNA rod. From the point of the biochemical interest in chromatin, an investigation of motions of the whole DNA rod will be important. Recently, Genest et al. (1982) and Wang et al. (1982) studied the dynamics of DNA in a core particle by using anisotropy decay measurement of intercalated dyes and indicated that the torsional motion of DNA still exists. Independently, we measured the nanosecond anisotropy decay of ethidium bromide intercalated in core DNA, and we showed that the internal motion of DNA in a nucleosome core particle occurs to the same extent as the linker DNA in extended chromatin (Ashikawa et al., 1983). With regard to the internal motion of the linker DNA, Hurley et al. (1982) studied the motion of the linker DNA of chromatin by using electron paramagnetic resonance spectra of bound spin-labeled intercalating reagents. They reported fairly large torsional oscillations of linker DNA of H1,H5-depleted chromatin.

In the present work, we have extended our earlier work and analyzed the internal motion of DNA by using theoretical calculations. The analysis allows quantitative estimation of the mobility, or flexibility, of DNA in a core particle and in

† From The Institute of Physical and Chemical Research. Hirosawa 2-1, Wako-shi, Saitama 351, Japan (I.A., K.K., and A.I.), the Faculty of Pharmaceutical Sciences, University of Tokyo, Hongo, Bunkyo-ku, Tokyo 113, Japan (Y.N. and M.T.), the College of General Education, University of Tokyo, Megro-ku, Tokyo 153, Japan (K.W. and K.I.), and The Institute for Solid State Physics, University of Tokyo, Minato-ku, Tokyo 106, Japan (T.N.). *Received January 31, 1983.*

0006-2960/83/0422-6018$01.50/0

the linker region of chromatin. We also show that overall conformational changes of chromatin are reflected in the motions of linker DNA; flexibility of the linker DNA appears to be suppressed when extended chromatin turns to the solenoidal form.

Materials and Methods

Preparation of DNA and Chromatin. DNA was isolated from calf thymus by the method of Kay et al. (1952). The sedimentation coefficient of this DNA was 11–21 S in 5 mM tris(hydroxymethyl)aminomethane (Tris), 100 mM NaCl, and 1 mM ethylenediaminetetraacetic acid (EDTA), pH 7.5, and the molecular weight was considered to range from 2 million to 6 million. Protein contamination was estimated by the Lowry method to be below 1% by weight. Chromatin and nucleosome core particles were also prepared from calf thymus. Methods of preparation were already described (Watanabe & Iso, 1981; Ashikawa et al., 1982), and only a summary of the procedures is given here. For the preparation of nucleosome core particles, oligonucleosomes were isolated from nuclei after the nuclei were digested with micrococcal nuclease. After histone H1 was depleted, the chromatin was redigested with micrococcal nuclease and applied to a Sepharose 6B column. We obtained nucleosome core particles by collecting appropriate elute fractions. Further purification of this sample was carried out by centrifugation in a 5–20% linear sucrose gradient. For long chromatin, digestion of the nuclei was carried out very briefly, and isolated chromatin was applied to the same column. Only fractions eluted near the void volume were taken as a sample. The intactness of the histone proteins in these samples was analyzed by polyacrylamide gel electrophoresis; the core particles had DNA with 145 ± 5 base pairs (bp), and the chromatin had very long DNA.

Measurements of Fluorescence. Measurements of the time courses of fluorescence intensity and anisotropy were performed with a single photon counting apparatus. Details of this system were already described (Kinosita et al., 1981). Exciting pulses were obtained from a high-pressure H_2 lamp (half-width 1 ns), and the 520-nm component was selected by passing through a monochromator and a series of optical filters. To polarize the exciting pulses, a Glan polarizer was used. The sample cuvette (1 cm × 1 cm) was kept at 20 °C. Emitted fluorescence components above 560 nm at right angles to the exciting light were collected through cutoff filters, a polarizer, and a polarization scrambler. Two photomultiplier tubes (Hamamatsu R943-02) detected parallel ($I_\parallel$) and perpendicular ($I_\perp$) polarized components simultaneously. The filters completely blocked the scattered excitation light: samples without ethidium bromide gave negligible signals. For the measurement of the steady-state fluorescence, a Xenon lamp was used as the light source. The optical system was the same as that of the nanosecond measurements.

Buffer conditions of the samples were usually 1 or 5 mM Tris and 0.2 mM EDTA, pH 7.5, and the ionic strengths of the samples were adjusted by adding a NaCl solution of appropriate concentration. Concentrations of the samples were within 0.1–0.2 mg/mL. Ethidium bromide was added so that P/D ([phosphate]/[dye]) ranged between 1500 and 6000. At these low concentrations of the added dye, energy transfer between the intercalated dyes was determined to be negligible (see Results and Discussion). Fluorescence measurements were made at least 3 times for each sample, and the reproducibility of the decay curves and other observed values was checked every time.

From the obtained time courses of the two polarized components, $I_\parallel(t)$ and $I_\perp(t)$, the total fluorescence decay curve, $I_T(t)$, and the anisotropy decay curve, $R(t)$, were calculated as follows:

$$I_T(t) = I_\parallel(t) + 2I_\perp(t) \quad (1)$$

$$I_D(t) = I_\parallel(t) - I_\perp(t) \quad (2)$$

$$R(t) = I_D(t)/I_T(t) \quad (3)$$

Fluorescence lifetimes and correlation times of the motions were calculated by using a least-squares program, as briefly described below.

The true total fluorescence intensity decay, $I_T^*(t)$, and the true anisotropy decay, $r(t)$, are related to $I_T(t)$ and $I_D(t)$ in the following manner:

$$I_T(t) = \int_0^t g(t')I_T^*(t - t')\,dt' \quad (4)$$

$$I_D(t) = \int_0^t g(t')I_T^*(t - t')r(t - t')\,dt' \quad (5)$$

Here, $g(t)$ is the response function of our apparatus and obtained as a scattering light from Ludox of the exciting pulses. The profiles of the light pulses at the excitation wavelength (520 nm) and the emission wavelength (600 nm) were almost identical; when we used the light pulse of the 600-nm component for $g(t)$, the calculated lifetimes and correlation times did not change by more than 0.1 ns (lifetimes) or 1 ns (correlation times). We assume that $I_T^*(t)$ was approximated by

$$I_T^*(t) = \sum_i I_i \exp(-t/\tau_i) \quad (6)$$

and $r(t)$ by one of the theoretical expressions below (eq 9 or 10). Then, parameters in $I^*(t)$ and $r(t)$ were determined so as to minimize the following functions:

$$F_T \equiv \sum_t [[I_T(t_n) - I_T^{calcd}(t_n)]^2/I_T(t_n)] \quad (7)$$

$$F_D \equiv \sum_t [[I_D(t_n) - I_D^{calcd}(t_n)]^2/I_T(t_n)] \quad (8)$$

Analysis of the Internal Motion of DNA in Nucleosome Core Particles and Chromatin. In order to characterize the internal motion of DNA, we adopted the following analysis. For DNA in solution, we used the Barkley–Zimm formula (Barkley & Zimm, 1979), which represents the anisotropy decay originated from the torsional motion of DNA. Their model for the calculation is a uniform elastic rod of DNA with free ends to which the fluorophore is bound only at the center. The more general model of Allison & Schurr (1979) allows the fluorophore to be bound at any subunit with equal probability and accommodates arbitrary subunit lengths, including the uniform limit of zero subunit length. Thomas et al. (1980) have shown that the subunit length is sufficiently short (i.e., 20 bp) and that the fluorescence polarization anisotropy (FPA) data cannot distinguish the discrete from the uniform model. The expression we adopted is

$$r(t) = r_0[0.75 \exp[-(t/\alpha)^{1/2}] + 0.25] \quad (9)$$

with $\alpha = \pi^2 b^2 \eta C/(4k_B{}^2T^2)$ where k_B is the Boltzmann constant, T the absolute temperature, b the hydrodynamic radius of the model DNA, η the medium viscosity, and C the torsional rigidity of the DNA in the problem. One can obtain the torsional rigidity of the DNA by fitting eq 9 to the observed anisotropy decay curve.

In eq 9, the polar angle for the dye with respect to the helix axis (ϵ) is assumed to be 90° (Dickerson et al., 1982). Thomas et al. (1980) and Miller et al. (1982) used $\epsilon = 70.5°$ or 70° for the calculation of torsional rigidities. However, the value of this polar angle is not known rigorously now, and we cannot discriminate which value of ϵ (70° or 90°) is better to use. In

order to simplify calculations, we use $\epsilon = 90°$ in this paper. What we think most important in this paper is not the torsional rigidity of free DNA, which has been already reported by Thomas et al. (1980) and Millar et al. (1980, 1982), but comparison of the rigidity in core DNA or chromatin linker DNA with that of free DNA in solution. One can obtain the torsional rigidity of the DNA by fitting eq 9 to the observed anisotropy decay curve.

For DNA in a core particle and chromatin, the observed anisotropy decay, $r(t)$, is represented as follows:

$$r(t) = r_i(t)r_w(t) \tag{10}$$

In this expression, $r_w(t)$ is the time course of the anisotropy decay due to the rotation of the whole core particle or, in the case of chromatin, due to the movement of nucleosomes at the ends of the linker DNA in which the dye resides. We assume these motions to be isotropic, that is

$$r_w(t) = \exp(-t/\phi_2) \tag{11}$$

$r_i(t)$ is the time course of the anisotropy decay due only to the internal motion of DNA. As $r_i(t)$, eq 9 will probably be unsuitable, because in chromatin there must exist some ionic bonds of considerable rigidity between DNA and the histone proteins. We therefore calculated theoretical anisotropy decays for a DNA rod in which both ends are fixed. The rod was assumed to be uniform and elastic as in the Barkley–Zimm model. Details of the calculation and the obtained expressions are described in the Appendix. Since the exact equation was too complex for curve fitting, we used an approximate expression (see Appendix):

$$r_i(t) = r_0\{a_1 \exp[-(t/\phi_1)^{1/2}] + a_2\} \tag{12}$$

In this equation, parameters a_1 ($=1 - a_2$) and ϕ_1 are related to the length (L) between the fixed ends, the torsional rigidity (C) of the DNA rod, and the friction (ρ) per unit length of the DNA ($\rho = 4\pi b^2\eta$). In the least-squares analysis of experimental data, we fixed r_0 to 0.36, which is the same value as that in free DNA, since experimental $R(0)$ values for core particles and chromatin were always close to 0.36. This practice minimizes the number of adjustable parameters. When we did not fix r_0, the analysis sometimes gave a slightly larger value for r_0.

The least-squares analysis gave experimental parameters for the internal motion, a_1 and ϕ_1. These two parameters allow the estimation of L/C and $L\rho$ as shown in the Appendix. Individual values of L, C, and ρ (or the effective viscosity η), however, cannot be determined alone unless we make further assumptions. This is an inherent property of our model, for which the exact $r_i(t)$ values depends only on the combined quantities L/C and $L\rho$ (see Appendix).

Results and Discussion

Steady-State Anisotropy Values of Ethidium Bromide in DNA, Core Particles, and Chromatin. In the previous paper (Ashikawa et al., 1983), we showed a fluorescence anisotropy decay curve of ethidium in core DNA. We concluded that internal motions occur to some extent in core DNA. In this subsection, we examine the effect of energy transfer and confirm the above conclusion.

Figure 1 shows the observed steady-state anisotropy values of ethidium bromide intercalated in DNA and other samples for various D/P ([dye]/[phosphate of DNA]) values. Anisotropy values for long DNA and 146 bp DNA drop as the P/D value decreases. This is caused by the occurrence of energy transfer between intercalated ethidium molecules. We can estimate the fluorescence depolarization due purely to the

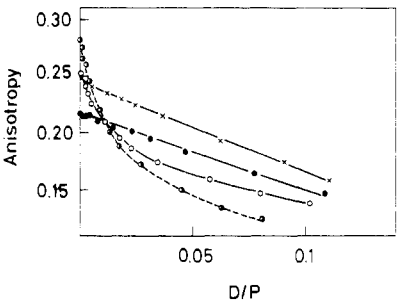

FIGURE 1: Steady-state fluorescence anisotropy values of ethidium intercalated in (×) long DNA. (●) 146 bp DNA, (○) nucleosome core particles, and (◑) chromatin. The abscissa represents the concentration of the added dye in terms of D/P ([dye]/[phosphate of DNA]). Sample concentrations were about 0.05 mg/mL, and measurements were performed in 5 mM Tris and 0.2 mM EDTA, pH 7.5 at 20 °C.

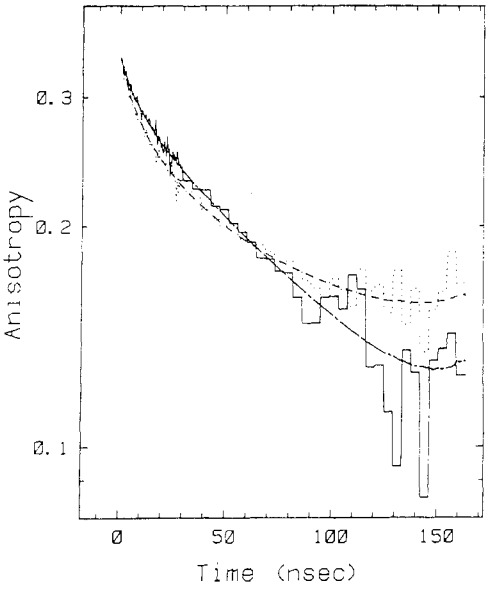

FIGURE 2: Fluorescence anisotropy decay curves of intercalated ethidium in long DNA (···) and nucleosome core DNA (—). Sample concentrations were 0.1–0.2 mg/mL, and measurements were performed in 5 mM Tris and 0.2 mM EDTA, pH 7.5 at 20 °C. P/D = 1500–3000. The anisotropy values after 30 ns are averaged over 10 channels; 1 ns equals 2.32 channels. (- - -) is the least-squares fitting curve with Barkley's formula (eq 9) to the decay of DNA in solution. (–·–) represents the result of a least-squares fit with eq 10–12 to the observed decay of DNA in nucleosome cores.

motions of the dye in DNA as the extrapolated value of P/D to infinity (that is, $D/P \sim 0$). On the other hand, as the P/D value decreases, the anisotropy values of ethidium intercalated in nucleosome cores and chromatin drop more rapidly than those of long DNA in solution. This phenomenon has already been reported by Wu et al. (1980) and Genest et al. (1981). They concluded that in nucleosome cores or chromatin, intercalated dyes are clustered and extensive energy transfer occurs between them.

Note in Figure 1 that the anisotropy value of ethidium in core particles extrapolated to a P/D of infinity, 0.25, is considerably lower than the r_0 of 0.36 for free DNA, a value that would be obtained in the absence of DNA motion (the r_0 of DNA in a core particle is almost the same as that in free DNA as seen in Figure 2). Of course, the rotation of the whole core decreases the steady-state anisotropy value. However, since the correlation time for the rotation of a core particle is considered to be 140–220 ns (see below), an anisotropy value higher than 0.31 is predicted in the absence of internal motions. The observed value of 0.25 indicates the existence of mobile

stretches of DNA in a core particle which presumably undergo torsional motions.

In the case of chromatin, added ethidium bromide has been shown to intercalate exclusively to the linker region (0.4–22 mM Na^+) (Paoletti et al., 1977; Erard et al., 1979; Genest et al., 1981) when the dye concentration is low. This fact holds for solenoidal chromatin in vivo (Cech & Karrer, 1980). In Figure 1, we find the extrapolated anisotropy value of the dye in chromatin to be 0.28, much lower than r_0. The difference suggests that the linker DNA also experiences internal (or torsional) motions.

Since the extrapolated anisotropy values for free DNA and core DNA are rather similar, one may suspect that the core sample might have contained a small amount of free DNA to which the added ethidium was bound. In order to eliminate this possibility, we measured the time dependence of the steady-state anisotropy value in the presence of 1 mM Ca^{2+} and micrococcal nuclease. While the steady-state anisotropy value of ethidium in free DNA dropped rapidly, the anisotropy value in core DNA remained almost unchanged. Ethidium in the core sample, therefore, was truely intercalated in the core DNA.

Nanosecond Fluorescence Anisotropy Decays for Free DNA and DNA in Nucleosome Core Particles. Figure 2 shows the fluorescence anisotropy decay curves of ethidium bromide intercalated in DNA around nucleosome cores (solid line) and in free DNA (dotted line). Solvent conditions of both samples were 5 mM Tris and 0.2 mM EDTA, pH 7.5. The anisotropy decay curve of the dye in long DNA (dotted line) was clearly approximated by eq 9 (- - -), with $r_0 = 0.357 \pm 0.002$ and $\alpha = 56.4 \pm 7.3$ ns (standard deviations of several measurements). From this correlation time, the torsional rigidity of this DNA is calculated to be $(2.04 \pm 0.27) \times 10^{-19}$ erg·cm. In this calculation, we take the hydrodynamic radius of DNA, b, to be 1.35 nm (Millar et al., 1982). The obtained torsional rigidity is somewhat larger than the value obtained by Thomas (1.29×10^{-19} erg·cm) and by Millar (1982) (1.43×10^{-19} erg·cm). The discrepancy may arise for several reasons. First, our experiments were performed in a solution of very low ionic strength where DNA is stiffer. Second, P/D values for our sample were very high as compared to those for the samples of Thomas and Millar, eliminating the possibility of energy transfer almost completely (cf. Figure 1). For samples with P/D of 100–200, we obtain torsional rigidity values close to 1.4×10^{-19} erg·cm. Third, we estimated the rigidity by using $\epsilon = 90°$ whereas Thomas et al. (1980) and Millar et al. (1982) estimated the rigidity by using $\epsilon = 70°$. If one calculates the torsional rigidity by using $\epsilon = 90°$, one must obtain a larger value than if one uses $\epsilon = 70°$. Fourth, Thomas et al. (1980) assumed that the hydrodynamic radius of DNA, b, was 1.2 nm. If we use their value for b, the calculated torsional rigidity increases by a factor of 1.27, because the torsional rigidity is inversely proportional to b^2. Our somewhat arbitrary choice of 1.35 nm for b, in the absence of a definite estimate, will not affect the discussion below in which we try to compare DNA in different form.

As discussed in the previous section, the anisotropy decay of fluorescence of ethidium bromide in core DNA is considered to result from both the rotation of the whole core and the internal motion of DNA in the core particle. We therefore analyzed the data with eq 10–12. The least-squares fitting curve is shown in Figure 2 (-·-); the fit is satisfactory. The calculated $r_i(t)$, i.e., eq 12, is shown in Figure 4 (solid line), and the correlation time ϕ_2 in eq 11 was calculated to be about 170 ns. This is a reasonable value for the rotation of a core particle. Previous studies (Dieterich et al., 1979), the anisotropy decay of a pyrene-labeled nucleosome core (I. Ashikawa et al., unpublished results), and the three dimensions of the core (Finch et al., 1981) suggest that the rotational correlation time of the core particle is within 140–220 ns. Also note that the rotation of an oblate spheroidal particle as the core (Finch et al., 1981) results in a practically single-exponential decay of anisotropy (Tao, 1969) as assumed in eq 11. When we changed the correlation time of the overall rotation (ϕ_2) within ±15% from the value of 170 ns, which was obtained from the least-squares calculation, deviations of the parameter values for the internal motion of DNA in a core particle (L/C and $L\eta$; see below) were found to be less than ±15%.

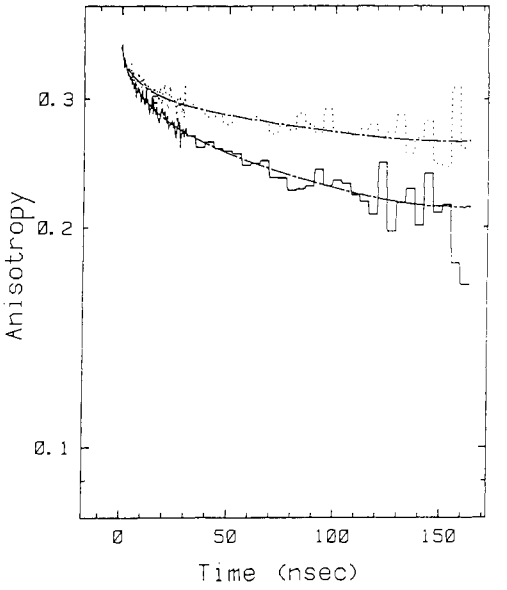

FIGURE 3: Fluorescence anisotropy decay curves of intercalated ethidium in chromatin DNA. Buffer conditions were 1 mM Tris and 0.2 mM EDTA, pH 7.5 (—), and 50 mM NaCl, 1 mM Tris, and 0.2 mM EDTA, pH 7.5 (···). The temperature in the cuvette was 20 °C. P/D = 2000–3000. (-·-) is the least-squares fit with eq 10–12 to the observed decays.

Nanosecond Fluorescence Anisotropy Studies of DNA in Long Chromatin. The structure of chromatin has been reported to change according to the ionic circumstances of the solvent and the presence of small amounts of Ca^{2+} or Mg^{2+} (Thoma et al., 1979). At moderate ionic strength (50–200 mM NaCl) or in the presence of Ca^{2+} or Mg^{2+} (greater than 1 mM), chromatin assumes a compacted form, which is called the "solenoid structure" (Finch & Klug, 1976), while at very low ionic strength and in the absence of divalent cations, it assumes an extended form, where core–core interaction is absent and the linker DNA is in the extended form. We investigated whether fluorescence depolarizations of ethidium in chromatin reflect the above-mentioned structural change. The dye concentration was kept low so that the fluorescence anisotropy reflected the mobility of the linker DNA.

The anisotropy decay curves of the dye in chromatin in 1 mM Tris and in 50 mM NaCl are shown in Figure 3. The decays of anisotropy in both samples are not as extensive as in the case of free DNA, the reason for which should be restriction of the internal motion and of the overall motion of the linker DNA. Both ends of about 30 bp of linker DNA are bound to the core protein or histone H1, and the torsional motion should not be completely free at these points.

Decay profiles of the two forms of chromatin in Figure 3 are different. The decay of chromatin in 50 mM NaCl is suppressed more than that in 1 mM Tris, and the anisotropy

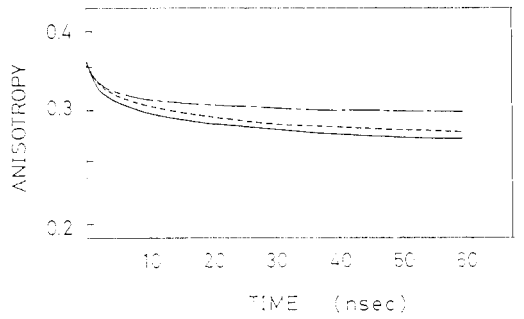

FIGURE 4: Calculated anisotropy decays, $r_i(t)$, of intercalated ethidium due only to the internal motion of DNA in core particles (—) that of linker DNA in extended chromatin (- - -), and that of linker DNA in condensed chromatin (—·—). These curves were obtained by fitting the observed decays (Figures 2 and 3) with eq 10, calculating the parameters in this equation, and depicting the curve following eq 12.

reaches an almost constant value beyond 50 ns. On the other hand, the anisotropy decay of extended chromatin in 1 mM Tris buffer drops faster than that of condensed chromatin and decays slowly even after 50 ns. These differences are supposed to result from the difference in the flexibility of the linker DNA and the nucleosome mobility between the two forms of chromatin.

In this case also, we decomposed the decay curves into the one corresponding to the internal motion, $r_i(t)$, and that resulting from the movement of nucleosomes in chromatin, $r_w(t)$, by fitting eq 10 to the observed decay curves in Figure 3. Resultant fitting curves are shown in Figure 3 (—·—) and the calculated decay curves for the internal motion, $r_i(t)$, are shown in Figure 4. From this figure, one can recognize that the internal motion of the linker DNA in condensed chromatin in 50 mM NaCl (—·—) is restricted more than that of the linker DNA in extended chromatin in 1 mM Tris (- - -). Calculated values of ϕ_2 in eq 11, that is, the effective correlation time for the overall rotation of the linker DNA in chromatin, are about 450 ns for the extended chromatin and about 1100 ns for the condensed chromatin. Although precision is not warranted for such large ϕ_2 values, the increase in ϕ_2 clearly indicates suppression of the movement of nucleosomes in chromatin accompanying the whole structural change of chromatin from the extended form to the condensed (or solenoidal) form.

The assumption of single-exponential decay for the overall rotation, eq 11, may appear too simplistic for the case of chromatin. Since the rotational correlation time for a free nucleosome core particle is expected to be greater than 140 ns as already discussed, the overall rotation must be characterized by correlation times greater than 140 ns. The fact that the fit with eq 10 is excellent (Figure 3), where ϕ_1 is much shorter than 140 ns (12.0 ns for the extended chromatin and 5.9 ns for the condensed chromatin), then suggests that eq 11 is adequate, at least to the first approximation, for the time range examined.

Characterization of the Internal Motion (or Torsional Motion) of DNA. We discuss here the torsional motion of DNA in a nucleosome core particle and in the linker region of chromatin. We assumed, as a model of calculation, a uniform rod of DNA with fixed ends. We do not know the actual binding site of ethidium in core DNA or linker DNA at present. In this paper, we took two binding modes of the dye into account: in one case, the dye was assumed to bind to the midpoint of the DNA with fixed ends, and in another case, the dye was assumed to bind uniformly to the DNA. Since the real binding mode (or the binding site) will be an intermediate of these two extremes, we discuss the torsional motion of DNA, considering these two binding mode (midpoint binding and average binding) independently. In this section, we assume that dye resides in the midpoint of the DNA in which both ends are fixed. In Figure 4, the asymptote at $t \rightarrow \infty$ is related to the standard deviation of the torsional angle, i.e., the extent of the torsional fluctuation, as shown in the Appendix. The estimated deviations are 17.9° for DNA in a core particle, 16.9° for the linker DNA in extended chromatin, and 11.6° for the linker DNA in condensed chromatin. Thus, the mobility of the linker DNA in condensed chromatin is lower than that in extended chromatin.

Table I: Obtained Relationships[a] among the Length (L), the Torsional Rigidity (C), and the Effective Viscosity (η) of Mobile DNA in Core Particles and Chromatin

	L/C (erg^{-1})	$L\eta$ (cm·P)
core DNA	1.1×10^{13} (1.6×10^{13})[b]	7.3×10^{-8} (7.3×10^{-8})
linker DNA, extended	1.0×10^{13} (1.5×10^{13})	9.5×10^{-8} (1.0×10^{-7})
linker DNA, condensed	7.1×10^{12} (1.1×10^{13})	7.5×10^{-8} (7.1×10^{-8})

[a] The radius of the DNA rod, b, was assumed to be 1.35 nm. [b] Values in parentheses were calculated with the assumption of random distribution of the dye in DNA.

Table II: Calculated Torsional Rigidities, Lengths, and Effective Viscosities for the Mobile Segment of DNA in Core Particles and Chromatin[a]

DNA	$C = 2.0 \times 10^{-19}$ $L > 1000$ $\eta = 0.01$		
core DNA	$C = 2.0 \times 10^{-19}$ $L = 65$ $\eta = 0.033$	$C = 1.6 \times 10^{-19}$ $L = 52$ $\eta = 0.041$	$C = 0.9 \times 10^{-19}$ $L = 30$ $\eta = 0.073$
linker DNA, extended	$C = 2.0 \times 10^{-19}$ $L = 60$ $\eta = 0.047$	$C = 1.6 \times 10^{-19}$ $L = 48$ $\eta = 0.058$	$C = 1.0 \times 10^{-19}$ $L = 30$ $\eta = 0.093$
linker DNA, condensed	$C = 2.9 \times 10^{-19}$ $L = 60$ $\eta = 0.037$	$C = 1.6 \times 10^{-19}$ $L = 33$ $\eta = 0.046$	$C = 1.4 \times 10^{-19}$ $L = 30$ $\eta = 0.073$

[a] Values in this table were calculated with the assumption of midpoint binding of the dye in DNA. If one assumes average binding of the dye, these values must be changed as mentioned in the text. Torsional rigidity (C) is in erg centimeters, length (L) is in base pairs, and effective viscosity (η) is in poise.

We can estimate the length, L, of the movable DNA segments, their torsional rigidity, C, and the effective friction (or the effective viscosity, η) on these segments according to the procedure described in the Appendix. However, as mentioned earlier, a number of parameters obtained from the observed decay curves are deficient for the settlement of these three parameters, and only the relationship between them can be determined. Calculated values of L/C and $L\eta$ are tabulated in Table I.

We estimate the parameters L, C, and η by using the obtained relationships and the restriction of these values inferred from results concerning DNA flexibility and the structure of chromatin. In the second column of Table II, we assume that the rigidity, C, is common to all DNAs except for the one in condensed chromatin, where the length, L, is fixed to the value obtained for extended chromatin. We think that these values are fairly reasonable, but these values are not the unique ones. The third column of Table II shows the calculated values in which the torsional rigidity of the DNA in the complex is assumed to be 80% of that of DNA in solution (5 mM Tris and 0.2 mM EDTA, pH 7.5). High ionic strength is known to reduce the rigidity by about 20% by screening the negative charges of the phosphate moieties of DNA (Millar et al., 1982). If the rigidity of DNA is not changed by being forced

to bend in a core particle, this value is considered to be the lower limit of the torsional rigidity. The fourth column of Table II shows the calculated values where the length of the movable segment is fixed at 30 bp. The length of the linker DNA of calf thymus chromatin has been considered to be about 30 bp (Weishet et al., 1979). We think that the length of core DNA between the ionic bonds will be several tens of base pairs. Values of the torsional rigidity in the fourth column (Table II) appear to be too small. In Table II, values of the effective viscosity are estimated to be from 3 to 5 times as large as that against free DNA. This probably results from the ionic bondings between DNA and the histone proteins.

Quite recently, Wang et al. (1982) reported the torsional rigidity of core DNA, and their value is 1.8×10^{-19} erg·cm. However, for $r_i(t)$, they used the Barkley and Zimm formula (eq 9), which can be applied only to DNA with free ends. Therefore, their treatment is not considered to be appropriate for the case of core DNA.

Characterization of the Internal Motion of DNA Using Genest's Model. In the previous section, we assumed that a dye situates in the midpoint of the DNA in which both ends are fixed. Genest et al. (1982) have studied the fluorescence anisotropy decay of ethidium in core DNA. In their paper, they extended the theory of Allison & Schurr (1979) to incorporate fixed-end boundary conditions. They assumed average binding of the dye to core DNA in contrast to our model mentioned in the previous section.

In this section, we analyze our fluorescence anisotropy data by using calculations similar to that of Genest et al.: random distribution of the dye molecule in the DNA rod. In this case also, we found that the approximate expression (eq 12) simulated very well the exact equation, and we have estimated L/C and $L\eta$ by using a procedure similar to that in the previous section. Calculated values of L/C and $L\eta$ for the case of random distribution of the dye are shown in parentheses in Table I. As seen in this table, the L/C values for average binding of ethidium are 1.5 times as large as that for midpoint binding. However, each $L\eta$ value is almost unchanged even if one assumes average binding.

One can estimate the parameters L, C, and η by using the relationships shown in Table I. In this case, if one assumes that L is the same as that in Table II, the value of C in Table II is reduced by a factor of 0.7 while η is unchanged. If one assumes that C is the same as that in Table II, the value of L is increased by a factor of 1.5, and the value of η is reduced by a factor of 0.7.

Genest et al. (1982) concluded in their paper that the length and torsional rigidity of the movable segment of DNA in a core particle are 15 bp and 4.08×10^{-20} erg·cm, respectively. However, they could fit their formula to only the first 20-ns portion of the observed decay curve, and we could fit our formula to the entire portion of the decay curve. Because the theoretical decay curves of ours in this section and theirs are the same, the observed decay curves of ours and theirs should be different.

Binding Mode of DNA to the Core Protein. As discussed above, if the torsional rigidity of DNA in a core particle is not reduced largely as compared to that of free DNA, the movable length will be longer than 50 bp. Because a core particle contains about 146 bp of DNA, a considerable portion of the core DNA seems to be movable with the torsional rigidity mentioned above. However, it is unreasonable that segments larger than 50 bp exist free from the ionic bondings with the histone octamer. Our result should be interpreted as follows. Ethidium dye will be intercalated to a rather free

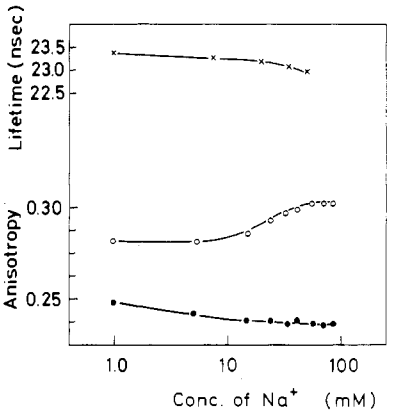

FIGURE 5: Fluorescence lifetimes (×) and steady-state anisotropy values of intercalated ethidium bromide in chromatin (○) and in free DNA (●) at various concentrations of NaCl. Buffer conditions were 1 mM Tris and 0.2 mM EDTA, pH 7.5, and concentrations of samples were 0.1 mg/mL for the lifetime measurements and 0.05 mg/mL for the steady-state anisotropy measurements. $P/D = 3000$; the temperature was held at 20 °C.

portion of the core DNA, the moiety of the intercalation site, whose length will be about several tens of base pairs, is in a relatively free state, and the ends of the DNA segment, where the ionic bonds with the histone protein exist, will reorient to some extent. Therefore, it looks as if the movable segment(s) contain(s) as much as greater than 50 bp.

In this case of the linker DNA, the movable segment does not seem to be limited to the 30 bp DNA in the linker portion, which has been thought to be relatively free sites according to the results of nuclease cutting (Weishet et al., 1979). At the entrance points of the linker DNA to the core region, there must exist ionic bonds of a certain strength with the core protein or histone H1. According to our results, probably even in these points the torsional motion of DNA is not suppressed completely but occurs to some extent. All these results indicate that the binding of DNA to the core protein is fairly soft.

As to the rigidity and the length of movable DNA in a core particle and chromatin, there may exist another explanation: the length is confined to about 30 bp, and the rigidity is reduced by a factor of 0.5 (Table II, fourth column). However such a large reduction in rigidity is rather unlikely at least for linker DNA in extended chromatin, whose conformation is considered to be almost same as that of free DNA. Further study is required to determine these values (L and C) uniquely.

Steady-State Fluorescence Anisotropy Change of Ethidium in Chromatin. It has been stated previously that the overall structural change of chromatin is reflected in the extent of mobility of the linker DNA. Using this property, we investigated the structural transition of chromatin accompanying an increase in the ionic strength of the solvents.

In Figure 5, open circles represent the steady-state anisotropy values of ethidium intercalated in the linker DNA at various NaCl concentrations. Motions of the linker DNA are suppressed when the NaCl concentration increases from 10 to 50 mM. On the other hand, closed circles represent the anisotropy values of the dye in long DNA. The change is in a direction opposite to the case of chromatin; free DNA becomes more mobile as the ionic strength increases.

The transition in the anisotropy value for the linker DNA occurs cooperatively in the range of 10–50 mM NaCl. Because an electron microscopy study by Thomas et al. (1979) indicated that the extended to condensed form transition occurs in the salt concentration range from 10 to 40 mM, the change in the anisotropy value is confirmed to reflect the whole structural change of chromatin. On the other hand, Butler

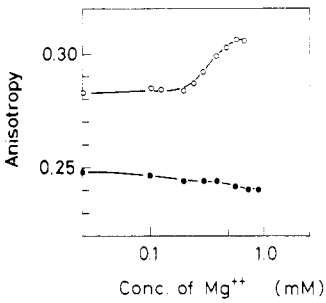

FIGURE 6: Steady-state fluorescence anisotropy values of ethidium in chromatin (○) and in free DNA (●) at various molar concentrations of $MgCl_2$. Measurements were performed in 1 mM Tris and 0.2 mM EDTA, pH 7.5 at 20 °C. Sample concentrations were about 0.05 mg/mL. P/D = 3000.

& Thomas (1980) studied the structural transition of chromatin using sedimentation velocity and reported that the transition is linear with salt concentration between 5 and 140 mM NaCl. Their result indicates that the whole structural change of chromatin proceeds linearly with an increase of the ionic strength of the solvent. If one considers our results and theirs, the motions of the linker DNA are suppressed when a solenoidal structure of some extent of rigidity is formed.

Figure 6 shows the steady-state anisotropy values of ethidium in chromatin at various concentrations of Mg^{2+} in solution. The anisotropy increases with Mg^{2+} concentration in the range from 0.5 to 1 mM, and we can recognize that motions of the linker DNA are suppressed above this Mg^{2+} concentration range. Thoma et al. (1979) also reported that the structural change of chromatin to the solenoidal form occurs in this Mg^{2+} concentration range, and these data also confirm that the whole structural change of chromatin is reflected in the mobility of the linker DNA.

Lifetimes of Ethidium in DNA, Nucleosome Cores, and Chromatin. In this subsection, we discuss whether the conformational state of DNA is reflected in the fluorescence lifetime of the intercalated dye. Figure 7 shows an example of the decay of the observed total fluorescence intensity, $I_T(t)$, together with a calculated best-fit single-exponential decay and corresponding weighted residuals. The single-exponential approximation appears to be satisfactory. Other samples gave similar residuals.

The lifetime of the dye in free DNA is 23.24 ± 0.10 ns, while that in DNA in core particles is 22.58 ± 0.08 ns. These values do not change within experimental error when P/D values are increased by 15-fold. In the case of the linker DNA in chromatin, calculated lifetimes are 23.45 ± 0.08 ns for the measurements in 1 mM Tris and 0.2 mM EDTA, pH 7.5, and 23.09 ± 0.09 ns for the measurements in 50 mM NaCl, 1 mM Tris, and 0.2 mM EDTA, pH 7.5. The lifetime values of intercalated ethidium are plotted against the ionic strength of the solution in Figure 5. The lifetime decreases in the range of 10–50 mM, where the structure of chromatin changes. Thus, the differences of the lifetime values may reflect the conformational variations among free DNA, core DNA, and linker DNA; modes of base stacking in these DNAs are slightly different from one another. It is considered that when DNA is forced to bend, as may well be the case for the core DNA or the linker DNA in condensed chromatin, the interaction between the bases and the intercalated dye is somewhat weakened, resulting in a slightly shorter lifetime.

Conclusions

Klug et al. (1980) and Finch et al. (1981) have studied the structure of core particles and the histone octamer by X-ray

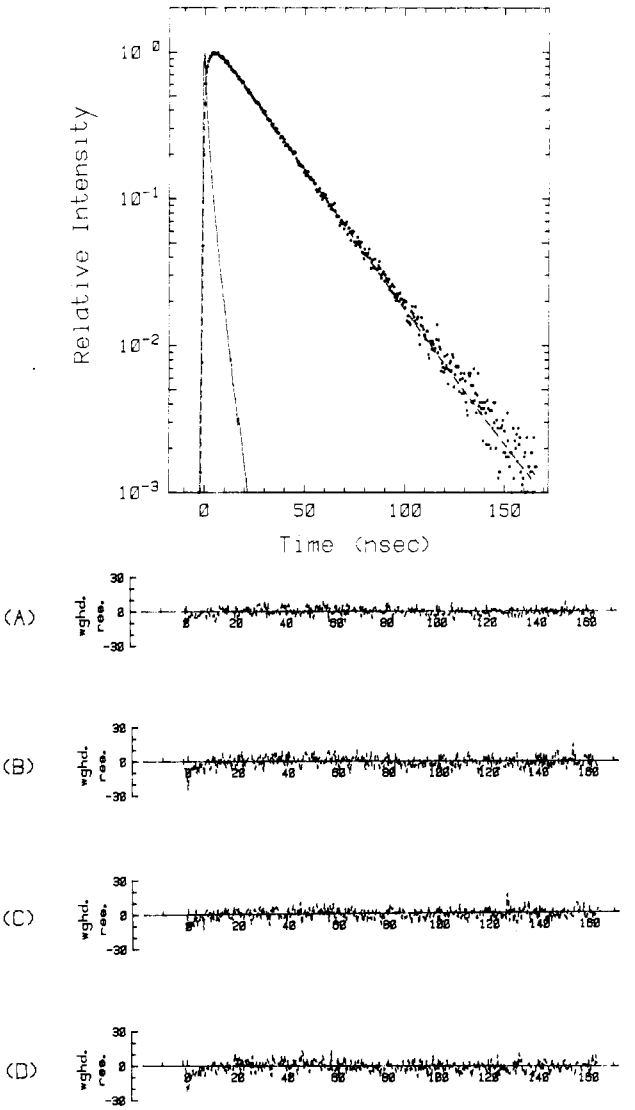

FIGURE 7: (Top) Fluorescence intensity decay of intercalated ethidium in nucleosome core DNA. (–·–) represents the response function $g(t)$; (– – –) represents the result of a least-squares fit with a single-exponential decay form. (Bottom) The weighted residuals of the single-exponential fit to the observed intensity decays of ethidium intercalated in (A) DNA in solution, (B) DNA in core particles, (C) linker DNA in extended chromatin, and (D) linker DNA in condensed chromatin. The measurement conditions were mentioned in the legends of Figures 2 and 3.

diffraction and image reconstruction. They suggested that the DNA in a core particle is fixed only at a few points, and not all around, and that the remaining portions are relatively free. Our results basically support their suggestions. Furthermore, the estimated length of the mobile DNA segment in a core particle indicates that the torsional motion at the "fixed" points is not suppressed completely. The calculated torsional rigidity, on the other hand, is almost the same as, or somewhat smaller than, that of free DNA. This finding may be significant for the mechanisms of replication or transcription of DNA around a core particle. The above conclusions have been drawn under the assumption that the internal motion of DNA in a core particle is mainly the torsional type. Further study is required to eliminate the possibilities of bending motions of the DNA or a segmental flexibility of the core particle.

As to the linker DNA in chromatin, if the binding mode of DNA to core protein or histone H1 is not so changed, the torsional stiffness increases as the structure of chromatin turns from an extended form to a solenoidal one. The linker DNA

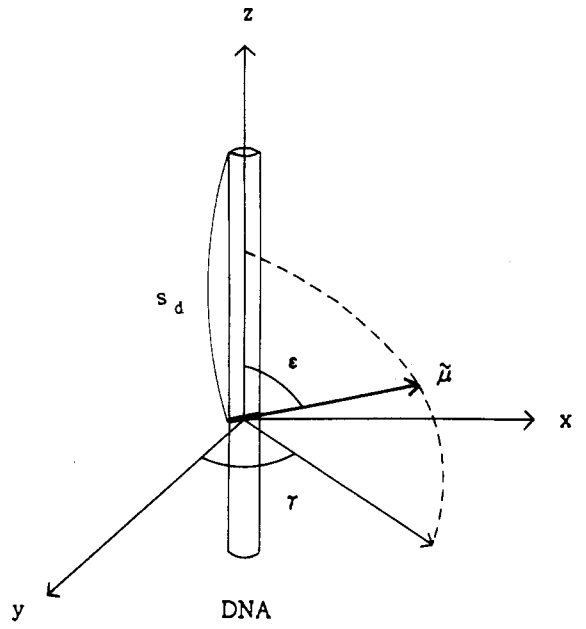

FIGURE 8: Model for the calculation of the anisotropy decay of a intercalated dye in DNA in which both ends are fixed. $\tilde{\mu}$ is a unit vector which represents the direction of the emission transition moment of the dye.

in solenoidal chromatin appears to be stiffer than the core DNA (Table II). Bending of the linker DNA accompanying the solenoid formation may be the cause of the increased torsional rigidity. Several models concerning the conformation or course of the linker DNA in solenoidal chromatin have been published (Worcel & Benyajati, 1977; Thoma et al., 1979; Mcghee et al., 1980), and we think that in the models of the solenoidal chromatin the linker DNA should be severely deformed from the extended conformation.

Appendix

Calculation of the Anisotropy Decay for the Torsional Motion of DNA with Fixed Ends. We assume the DNA in question to be an elastic rod with length L and with fixed ends and a dye to be situated at a distance s_d from one end. ϵ is the angle between the axis of DNA and the transition moments of excitation and emission (Figure 8). We assume that the directions of the transition moments of excitation and emission of ethidium are parallel (Millar et al., 1980). Let the direction of the emission transition moment of the dye at time zero be represented by the unit vector $\tilde{\mu}_0$ and that after time t by $\tilde{\mu}$. Then the anisotropy decay of fluorescence of the dye is written as follows (Kinosita et al., 1977):

$$r(t)/r_0 = \int\int w^s(\tilde{\mu}_0) P_2(\tilde{\mu}_0 \cdot \tilde{\mu}) g(\tilde{\mu}_0, 0|\tilde{\mu}, t)\, d\tilde{\mu}\, d\tilde{\mu}_0 \qquad \text{(A1)}$$

where $w^s(\tilde{\mu}_0)$ represents the stationary distribution of the direction of the emission transition moment in a local coordinate system (xyz in Figure 8) with the origin at the dye position and the xz plane containing the equilibrium orientation of $\tilde{\mu}$. P_2 is the second Legendre polynomial, that is, $P_2(\tilde{\mu}_0 \cdot \tilde{\mu}) = [3 \cos^2 (\tilde{\mu}_0 \cdot \tilde{\mu}) - 1]/2$. $g(\tilde{\mu}_0, 0|\tilde{\mu}, t)$ represents the probability that the dye with orientation $\tilde{\mu}_0$ at time zero will rotate into a new orientation $\tilde{\mu}$ by time t.

For the calculation of w^s and g, we adopted the procedure developed by Barkley & Zimm (1979). When both ends of DNA are fixed, the relative rotation angle of the cross section at a distance s from one end, $\gamma(s,t)$, is represented as follows:

$$\tau(s,t) = (2/L)^{1/2} \sum_{k=1}^{\infty} \xi_k \sin \lambda_k s \qquad \text{(A2)}$$

with $\lambda_k = k\pi/L$. The azimuthal (torsional) angle of $\tilde{\mu}$, $\gamma \equiv \gamma(s_d,t)$, in the DNA rod is then given by

$$\gamma = (2/L)^{1/2} \sum_{k=1}^{\infty} \xi_k \sin \lambda_k s_d \equiv \sum_{k=1}^{\infty} C_k \xi_k \qquad \text{(A3)}$$

Neglecting the polar angle which is fixed to ϵ, we obtain for w^s and g in eq A1

$$w^s(\gamma_0) = \delta(C_k \xi_k^0 - \gamma_0) \prod_{k=1}^{\infty} \phi_k^0(\xi_k^0) \qquad \text{(A4)}$$

$$g(\gamma_0, 0|\gamma, t) = \delta(C_k \xi_k^0 - \gamma_0) \prod_{k=1}^{\infty} \phi_k^f(\xi_k, t; \xi_k^0) \qquad \text{(A5)}$$

where $\phi_k^0(\xi^0)$ and $\phi_k^f(\xi_k,t;\xi_k^0)$ are given by eq II.23 and II.18 in Barlkey's paper (1979). Putting eq A4 and A5 into eq A1 and noting that $\tilde{\mu}_0 \cdot \tilde{\mu} = \sin^2 \epsilon \cos(\gamma - \gamma_0) + \cos \epsilon^2$, we finally obtained

$$r(t)/r_0 = (1 - \tfrac{3}{2}p^2)^2 + \tfrac{3}{4}p^4 e^{-\Gamma} + 3p^2(1 - p^2)e^{-\Gamma/4} \qquad \text{(A6)}$$

with

$$\Gamma(t) = [8DL/(\sigma\pi^2)] \sum_{k=1}^{\infty} [(\sin^2 \pi k\beta)^2/k^2][1 - \exp(-\sigma\pi^2 k^2 t/L^2)] \qquad \text{(A7)}$$

where $D = k_B T/\rho$, $\beta = \chi_d/L$, $\sigma = C/\rho$, and $p = \sin \epsilon$. In this equation, k_B is Boltzmann's constant, T is the absolute temperature, C is the torsional rigidity of the DNA rod, and ρ is the friction per unit length ($\rho = 4\pi\eta b^2$). Note that L, C, and ρ are not mutually independent in eq A7: $\Gamma(t)$ is a function of C/L and $L\rho$. For B-form DNA, we assumed p to be about 1.0 (Dickerson et al., 1982), and eq A6 is simplified as follows:

$$r(t)/r_0 = 0.75 \exp(-\Gamma) + 0.25 \qquad \text{(A8)}$$

In the analysis presented in the text, we take two cases into account: in one case, we assumed the dye to be situated at the midpoint of the DNA rod, that is, $\beta = 0.5$. In the other case, we assumed the dye to distribute randomly in the DNA rod; we integrate eq A7 from $\beta = 0$ to $\beta = 1$.

At equilibrium ($t \rightarrow \infty$), $\Gamma(t)$ approaches a constant value, $\Gamma(\infty)$, where $\Gamma(\infty) = (4k_B TL/C)[\beta(1 - \beta)]$ or $\Gamma(\infty) = k_B TL/C$ (for $\beta = 0.5$). For random distribution of β

$$\Gamma(\infty) = 0.67 k_B TL/C \qquad \text{(A9)}$$

and $\Gamma(\infty)$ can be obtained from the observed decay curves. The standard deviation, $\langle\gamma^2\rangle^{1/2}$, of the torsional angle is found to be $\Gamma(\infty)/2^{1/2}$.

Genest et al. (1982) calculated the fluorescence anisotropy decay of a dye in DNA with fixed ends by using a model similar to that used by Allison & Schurr (1979). They assumed a uniform distribution of the dye along the DNA rod. Their result is essentially identical with ours of the random distribution of β.

Since eq A7 and A8 are too complex for analysis of the experimental data, we approximated eq A8 with

$$r_i(t) = r_0\{a_1 \exp[-(t/\phi_1)^{1/2}] + a_2\} \qquad \text{(A10)}$$

where $a_2 = 0.75 \exp[-\Gamma(\infty)] + 0.25$, $a_1 = 1 - a_2$, and ϕ_1 is a parameter that depends on $C/(L^2\rho)$. The relation between ϕ_1 and $C/(L^2\rho)$ was determined numerically by curve fitting eq A10 to A8. As shown in Figure 9, this expression (dashed line) is able to simulate fairly well the exact solution for midpoint binding of ethidium (eq A8) for any combinations of length and torsional rigidity of DNA. Considering the number of parameters which must be determined is 2, we think

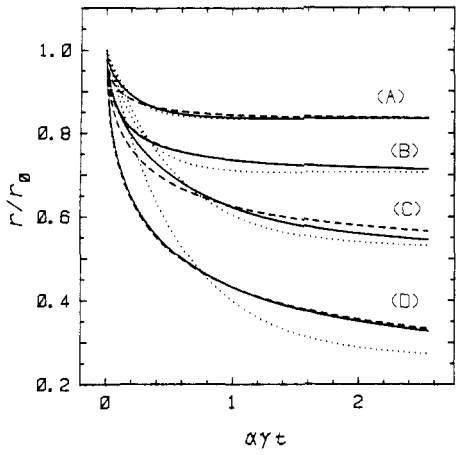

FIGURE 9: Least-squares fitting curves with eq A10 (---) and eq A11 (···) to the normalized anisotropy decay curves representing the exact solution (eq A7 and A8). In these fittings, we assumed that the dye was situated at the midpoint of the DNA. The abscissa is a normalized time, $\alpha\gamma t = \pi^2 k_B T t/(L\rho)$. With this time scale, eq A7 and A8 can be expressed by only γ ($=k_B TL/C$) and β ($=s_d/L$). The values used for the solid lines are (A) $\gamma = 0.25$ and $\beta = 0.5$, (B) $\gamma = 1.0$ and $\beta = 0.146$, (C) $\gamma = 1.0$ and $\beta = 0.5$, and (D) $\gamma = 4.0$ and $\beta = 0.5$. One can recognize in this figure that eq A10 is a relatively good approximation while the fit with eq A11 is poor. In the case of random distribution of the dye, fitting with eq 10 to the exact solution was much better. (Fitting curves are not shown here.)

that such a level of fitting as this will be satisfactory. In the case of average binding of the dye, the simulations are much better. The dotted lines in Figure 9 represent the fitting curves with the expression

$$r(t) = r_0[a_1 \exp(-t/\phi_1) + a_2] \qquad \text{(A11)}$$

This expression has usually been used for the anisotropy decay of restricted motions (Kinosita et al., 1977). However, in the case of the torsional motion of DNA, this expression fails to be a good approximation.

References

Allison, S. A., & Schurr, J. M. (1979) *Chem. Phys. 41*, 35–59.

Allison, S. A., Shibata, J. H., Wilcoxon, J., & Schurr, J. M. (1982) *Biopolymers 21*, 729–762.

Ashikawa, I., Nishimura, Y., Tsuboi, M., Watanabe, K., & Iso, K. (1982) *J. Biochem. (Tokyo) 91*, 2047–2055.

Ashikawa, I., Kinosita, K., Jr., Ikegami, A., Nishimura, Y., Tsuboi, M., Watanabe, K., & Iso, K. (1983) *J. Biochem. (Tokyo) 93*, 665–668.

Barkley, M. D., & Zimm, B. H. (1979) *J. Chem. Phys. 70*, 2991–3007.

Bolton, P. H., & James, T. L. (1980) *J. Am. Chem. Soc. 102*, 25–31.

Butler, P. J. G., & Thomas, J. O. (1980) *J. Mol. Biol. 140*, 505–529.

Cech, T. R., & Karrer, K. M. (1980) *J. Mol. Biol. 136*, 395–416.

Dickerson, R. E., Drew, H. R., Conner, B. N., Wing, R. M., Fratini, A. V., & Kopka, M. L. (1982) *Science (Washington, D.C.) 216*, 475–485.

Dieterich, A. E., Axel, R., & Cantor, C. R. (1979) *J. Mol. Biol. 129*, 587–602.

Early, T. A., & Kearns, D. R. (1979) *Proc. Natl. Acad. Sci. U.S.A. 76*, 4170–4174.

Erard, M., Das, G. C., de Murcia, G., Mazen, A., Pouyet, J., Chanpagne, M., & Daune, M. (1979) *Nucleic Acids Res. 6*, 3231–3252.

Finch, J. T., & Klug, A. (1976) *Proc. Natl. Acad. Sci. U.S.A. 73*, 1897–1901.

Finch, J. T., Brown, R. S., Rhodes, D., Richmond, T., Rushton, B., Lutter, L. C., & Klug, A. (1981) *J. Mol. Biol. 145*, 757–769.

Genest, D., Sabeur, G., Wahl, P., & Auchet, J.-C. (1981) *Biophys. Chem. 13*, 77–87.

Genest, D., Wahl, Ph., Erard, M., Champagne, M., & Daune, M. (1982) *Biochimie 64*, 419–427.

Hogan, M. E., & Jardetzky, O. (1979) *Proc. Natl. Acad. Sci. U.S.A. 79*, 6341–6345.

Hogan, M. E., & Jardetzky, O. (1980a) *Biochemistry 19*, 2079–2085.

Hogan, M. E., & Jardetzky, O. (1980b) *Biochemistry 19*, 3460–3468.

Hogan, M., Wang, J., Austin, R. H., Monitto, C. L., & Hershkowitz, S. (1982) *Proc. Natl. Acad. Sci. U.S.A. 79*, 3518–3522.

Hurley, I., Osei-Gyimah, P., Archer, S., Scholes, C. P., & Lerman, L. S. (1982) *Biochemistry 21*, 4999–5009.

Kay, E. R. M., Simmons, N. S., & Dounce, A. L. (1952) *J. Am. Chem. Soc. 74*, 1724–1726.

Kinosita, K., Jr., Kawato, S., & Ikegami, A. (1977) *Biophys. J. 20*, 289–305.

Kinosita, K., Jr., Kataoka, R., Kimura, M., Gotoh, O., & Ikegami, A. (1981) *Biochemistry 20*, 4270–4277.

Klevan, L., Armitage, I. M., & Crothers, D. M. (1979) *Nucleic Acids Res. 6*, 1607–1616.

Klug, A., Rhodes, D., Smith, J., Finch, J. T., & Thomas, J. O. (1980) *Nature (London) 287*, 509–516.

Kornberg, R. D. (1977) *Annu. Rev. Biochem. 46*, 931–954.

Mcghee, J. D., Rau, D. C., Charney, E., & Felsenfeld, G. (1980) *Cell (Cambridge, Mass.) 22*, 87–96.

Millar, D. P., Robbins, R. J., & Zewail, A. H. (1980) *Proc. Natl. Acad. Sci. U.S.A. 77*, 5593–5597.

Millar, D. P., Robbins, R. J., & Zewail, A. H. (1982) *J. Chem. Phys. 76*, 2080–2094.

Opella, S. J., Wise, W. B., & DiVerdi, J. A. (1981) *Biochemistry 20*, 284–290.

Paoletti, J., Magee, B. B., & Magee, P. T. (1977) *Biochemistry 16*, 351–357.

Robinson, B. H., Lerman, L. S., Beth, A. H., Fisch, H. L., Dalton, L. R., & Auer, C. (1980) *J. Mol. Biol. 139*, 19–44.

Shindo, H., Mcghee, J. D., & Cohen, J. S. (1980) *Biopolymers 19*, 523–537.

Tao, T. (1969) *Biopolymers 8*, 609–632.

Thoma, F., Koller, Th., & Klug, A. (1979) *J. Cell Biol. 83*, 403–427.

Thomas, J. C., Allison, S. A., Appellof, C. J., & Schurr, J. M. (1980) *Biophys. Chem. 12*, 177–188.

Wahl, Ph., Paoletti, J., & LePeqcq, J.-B. (1970) *Proc. Natl. Acad. Sci. U.S.A. 65*, 417–421.

Wang, J., Hogan, M., & Austin, R. H. (1982) *Proc. Natl. Acad. Sci. U.S.A. 79*, 5896–5900.

Watanabe, K., & Iso, K. (1981) *J. Mol. Biol. 151*, 143–163.

Weishet, W. O., Allen, J. R., Riedel, G., & Van Holde, K. E. (1979) *Nucleic Acids Res. 6*, 1843–1862.

Worcell, A., & Benyajati, C. (1977) *Cell (Cambridge, Mass.) 12*, 83–100.

Wu, H.-M., Dattagupta, N., Hogan, M., & Crothers, D. M. (1980) *Biochemistry 19*, 626–634.